OPEN

Prediction of malignancy for solitary pulmonary nodules based on imaging, clinical characteristics and tumor marker levels

Hongjun Hou, Shui Yu, Zushan Xu, Hongsheng Zhang, Jie Liu and Wenjun Zhang

Objective **To establish a prediction model of malignancy for solitary pulmonary nodules (SPNs) on the basis of imaging, clinical characteristics and tumor marker levels.**

Methods **Totally, 341 cases of SPNs were enrolled in this retrospective study, in which 70% were selected as the training group (n=238) and the rest 30% as the verification group (n=103). The imaging, clinical characteristics and tumor marker levels of patients with benign and malignant SPNs were compared. Influencing factors were identified using multivariate logistic regression analysis. The model was assessed by the area under the curve (AUC) of the receiver operating characteristic curve.**

Results **Differences were evident between patients with benign and malignant SPNs in age, gender, smoking history, carcinoembryonic antigen (CEA), neuron-specific enolase, nodule location, edge smoothing, spiculation, lobulation, vascular convergence sign, air bronchogram, ground-glass opacity, vacuole sign and calcification (all P<0.05). Influencing factors for malignancy included age, gender, nodule location, spiculation, vacuole sign and CEA (all P<0.05). The established model was as follows: Y=−5.368+0.055×age+1.012×gender (female=1, male=0)+1.302×nodule location (right upper lobe=1, others=0)+1.208×spiculation (yes=1, no=0)+2.164×vacuole sign (yes=1, no=0) −0.054×CEA. The AUC of the model with CEA was 0.818 (95% confidence interval, 0.763–0.865), with a sensitivity of 64.80% and a specificity of 84.96%, and the stability was better through internal verification.**

Conclusions **The prediction model established in our study exhibits better accuracy and internal stability in predicting the probability of malignancy for SPNs.**

European Journal of Cancer Prevention **30: 382–388**

European Journal of Cancer Prevention 2021, **30**:382–388

Keywords: computerized tomography, prediction model, solitary pulmonary nodule, tumor markers

Imaging Department, Weihai Central Hospital, Weihai, Shandong, China

Correspondence to Hongjun Hou, MB, Imaging Department, Weihai Central Hospital, West No. 3, East Mishan Road, Wendeng District, Weihai 264400, Shandong, China
Tel: +86 18306307538; e-mail: houhjdoctor409@163.com

Received 30 July 2020 **Accepted** 17 September 2020

Introduction

A solitary pulmonary nodule (SPN) refers to a single, round radiologic opacity that is not more than 3 cm in its maximum diameter and at least moderately well marginated, without distal atelectasis, pleural effusion, local lymph node enlargement and peripheral satellite lesions (Patel *et al.*, 2013; Truong *et al.*, 2014). The SPN frequently encountered on chest imaging may be solid or subsolid in attenuation. Subsolid nodules containing a component with ground-glass attenuation are highly likely to develop into premalignant or malignant lesions after the presence of 3–6 months (Naidich *et al.*, 2013; Borghesi *et al.*, 2020). Eight large trials of lung cancer screening suggested that the prevalence of at least one SPN ranged from 8 to 51%, and that of malignancy in patients with an SPN varied from 1.1 to 12.0% (Wahidi *et al.*, 2007). With the development of imaging technology and growing interest in lung cancer screening, the detection of SPNs has increased markedly. How to characterize and treat SPNs becomes a major concern for clinicians.

Multidetector computerized tomography (MDCT) plays an important role in assessing the morphological characteristics and nodal growth on serial images. It improves the specificity and sensitivity in the detection of pulmonary nodules by reducing misregistration artifacts and increasing spatial and contrast resolution, which provides more accurate characterization of nodules (Truong *et al.*, 2014; Snoeckx *et al.*, 2018). As reported in the various guidelines for pulmonary nodules, the nodule size and morphological characteristics are closely associated with the probability of malignancy (MacMahon *et al.*, 2005; Callister *et al.*, 2015; MacMahon *et al.*, 2017). Additionally, the clinical context should not be neglected when the probability of malignancy is assessed (Larici *et al.*, 2017). There is evidence suggesting that the probability of malignancy for SPNs may be increased in patients with advanced

0959-8278 Copyright © 2020 The Author(s). Published by Wolters Kluwer Health, Inc. DOI: 10.1097/CEJ.0000000000000637

age, smoking and history of extrathoracic malignant neoplasm (Kikano *et al.*, 2015). Although multiple prediction models of malignancy for SPNs have been established currently, including Veterans Affairs model, Mayo Clinic model and Brock model, serum tumor markers are almost missing in these models (Swensen *et al.*, 1997; Gould *et al.*, 2007; Chung *et al.*, 2018).

It is well-known that the detection of serum tumor markers contributes to the screening and early diagnosis of lung cancer. By measuring the tumor marker levels in patients with pulmonary nodules, Li *et al.*, found that the levels of serum cytokeratin fragment antigen 21-1 (CYFRA21-1) and carcinoembryonic antigen (CEA) were increased significantly in patients with malignant nodules when compared with those with benign nodules, suggesting a potential effect of serum tumor markers in determining benign and malignant pulmonary nodules (Li *et al.*, 2017). In this study, a prediction model of malignancy for SPNs was developed to assist the clinicians to effectively diagnose and treat SPNs based on the imaging features obtained from MDCT, clinical characteristics and serum tumor markers.

Methods

Study population

Between 1 July 2017 and 31 December 2019, totally 341 cases of SPNs who underwent surgical excision or puncture biopsy at Weihai Central Hospital were enrolled in this retrospective study. This study was performed on the basis of the principle of Helsinki Declaration and was approved by the Institutional Review Board of Weihai Central Hospital (approval no.: WHSZXYYKYLL-2020-03).

The included patients must meet all the following requirements, including: (1) the nodule diameter ≤3.0 cm, and no pulmonary atelectasis, pneumonia, satellite lesions and local lymph node enlargement; (2) able to cooperate better and almost keep the same breath-holding depth at each scanning; (3) complete pathological results and (4) the nature of nodule confirmed by pathological findings and clinical characteristics. Exclusion criteria were as follows: (1) patients with lung cancer-related symptoms, such as irritable cough, bloody sputum and chest pain, or those with local lymph node enlargement; (2) patients with obvious damage or severe insufficiency of important organs like the heart, liver and kidney; (3) pregnant women; (4) patients with a metal stent or internal fixator in the chest-back area, or those with common contraindications to iodinated contrast agents; (5) patients with SPNs extremely close to the heart margin or diaphragm and (6) patients taking other trial drugs 1 month before enrollment or participating in other trials.

Image acquisition

The thin-section computed tomography (CT) scanning was performed on the patient's chest using the GE BrightSpeed 16-layer MDCT scanner. The lung window (window level: -400HU; window width: 500HU) and mediastinal window (window level: 50HU; window width: 500HU) were set, respectively, and the section thickness was 1.25 mm. Additionally, 50 mL of iodinated contrast agent (300 mg I/mL) was injected in superficial veins of the forearm using a high-pressure injector, with a flow rate of 4 mL/s. The lesions were dynamically scanned at 30 s and 50 s after the injection of iodinated contrast agent, and the prolonged time of scanning was 5.6 s.

For each patient, two imaging specialists were independently responsible for reading the film and carefully recording the CT features of pulmonary nodules, including: (1) nodule location; (2) nodule size, namely the maximum diameter of nodule measured in the lung window; (3) edge features, such as smoothing, spiculation, lobulation, pleural indentation, vascular convergence sign, etc. and (4) internal characteristics like cavity and calcification. If there existed conflicts about the description of nodules, the third imaging specialist would involve in determination.

Measurement of serum tumor markers

Before surgery and drug use, 5 mL of peripheral venous blood from fasting patients in the morning was drawn and centrifuged to collect serum samples, which were stored at −20°C. The levels of serum tumor markers CEA, neuron-specific enolase (NSE), CYFRA21-1, carbohydrate antigen 125 (CA125) and CA199 were detected using electrochemiluminescence assay, and the kits were provided by Roche Diagnostics Ltd., Shanghai. All the operations were implemented based on the kit instructions.

Statistical analysis

SAS software (version 9.4, SAS Institute Inc., North Carolina, USA.) was used for statistical analysis. The data with normal and abnormal distributions were described as the mean ± standard deviations ($\bar{x} \pm s$) using Student's *t*-test and the median and quartile [M (Q_{25}, Q_{75})] by Mann–Whitney U test, respectively. Categorical data were expressed as the number of cases and its proportion [n (%)] using the chi-square test or Fisher's exact test. For investigating the influencing factors for benign and malignant SPNs, the variables with significant difference in univariate analysis were enrolled into a multivariate logistic regression model through stepwise regression. A prediction model of malignancy for SPNs was established, which was assessed by the area under the curve (AUC) of the receiver operating characteristic (ROC) curve. A significant difference was shown at $P < 0.05$.

Results

Baseline information of study population

Totally, 341 patients with SPNs were enrolled in this study between 1 July 2017 and 31 December 2019, with the mean age of (59.53 ± 8.97) years. There were 172 males aged (60.02 ± 8.38) years and 169 females aged (59.04 ± 9.53) years. Among them, 162 cases suffered from benign nodules, whereas 179 from malignant nodules.

Of 341 patients, 70% were randomly selected as the training group ($n=238$) and the rest 30% were as the verification group ($n=103$). The baseline information of training and verification groups is compared in Table 1. It was found that the differences were not pronounced between two groups in age, gender, smoking history, history of malignant neoplasm and complication of other diseases ($P>0.05$), which suggested that the data of the verification group could be used to internally verify the prediction model established by the data of training group.

Clinical characteristics and tumor marker levels of patients with benign and malignant solitary pulmonary nodule

In total, 238 cases in the training group were at the age of (59.47 ± 9.00) years, including 113 males and 125 females. Among them, there were 113 cases of benign SPNs and 125 cases of malignant SPNs.

The clinical characteristics and serum tumor marker levels of patients with benign and malignant SPNs are listed in Table 2. The results showed that the age of patients with malignant SPNs was older than those with benign SPNs ($P=0.001$). Compared with those with benign SPNs, the patients with malignant SPNs had a higher proportion of females ($P=0.001$) and a lower proportion of smoking history ($P=0.002$). In terms of serum tumor markers, the patients with malignant SPNs had a lower CEA level ($P=0.033$) and a higher NSE level compared with those with benign SPNs ($P=0.028$). There was no statistical significance in serum CYFRA21-1, CA125 and CA199 levels ($P>0.05$).

Imaging features of patients with benign and malignant solitary pulmonary nodule

The imaging features of patients with benign and malignant SPNs are compared in Table 3. It was shown that the differences were apparent between the patients with benign and malignant SPNs in the nodule location, presence or absence of edge smoothing, spiculation, lobulation, vascular convergence sign, air bronchogram, ground-glass opacity, vacuole sign and calcification (all $P<0.05$).

Multivariate logistic regression analysis of benign and malignant solitary pulmonary nodule

As shown in Table 4, multivariate Logistic regression analysis exhibited that the age [odds ratio (OR), 1.056; 95% confidence interval (CI), 1.016–1.097; $P=0.005$], gender (OR, 2.750; 95% CI, 1.451–5.212; $P=0.002$), nodule location (OR, 3.677; 95% CI, 1.558–8.675; $P=0.003$), spiculation (OR, 3.347; 95% CI, 1.628–6.880; $P=0.001$) and vacuole sign (OR, 8.706; 95% CI, 3.765–20.134; $P<0.001$) were the independent risk factors for malignant SPNs, whereas serum CEA level (OR, 0.948; 95% CI, 0.905–0.993; $P=0.024$) was a protective factor. Based on this, a prediction model for the malignancy of SPNs was established, namely $Y=-5.368+0.055\times\text{age}+1.012\times\text{gender (female}=1,\ \text{male}=0)+1.302\times\text{nodule location (right upper lobe}=1,\ \text{others}=0)+1.208\times\text{spiculation (yes}=1,\ \text{no}=0)+2.164\times\text{vacuole sign (yes}=1,\text{no}=0)-0.054\times\text{CEA}$; $P=\frac{e^{Y}}{1+e^{Y}}$. The larger the P value, the greater the risk of malignancy.

Diagnostic value and validation of the model

The diagnostic values of the age, CEA level, and models with CEA and without CEA are compared in Table 5. It can be observed that the model with CEA had a sensitivity of 64.80% and specificity of 84.96%, with the cut-off value of 0.61, and its AUC was 0.818 (95% CI, 0.763–0.865), significantly larger than 0.793 of the model without CEA (95% CI, 0.736–0.842; $P=0.029$), 0.621 of the age alone (95% CI, 0.556–0.683; $P<0.001$), and 0.580 of the CEA level alone (95% CI, 0.515–0.643; $P<0.001$). Figure 1 represents the ROC curves of each model. The internal verification of the model was performed using the data of the verification group. No significant difference was presented between the predictive number and actual number of the model with CEA in predicting malignant SNPs ($P=0.384$, Table 6), suggesting that this prediction model had better internal stability.

Table 1 Baseline information of training and verification groups, *n* (%)

Variables	Number of cases	Training group ($n=238$)	Verification group ($n=103$)	Z/χ^2	P value
Age, years, M (Q_{25}, Q_{75})		60 (55, 65)	59 (53, 66)	–0.474	0.635
Gender				2.763	0.096
Male	172	113 (47.48)	59 (57.28)		
Female	169	125 (52.52)	44 (42.72)		
Smoking history				3.537	0.060
No	230	168 (70.59)	62 (60.19)		
Yes	111	70 (29.41)	41 (39.81)		
History of malignant neoplasm				–	0.587
No	337	236 (99.16)	101 (98.06)		
Yes	4	2 (0.84)	2 (1.94)		
Comorbidity				0.524	0.469
No	239	164 (68.91)	75 (72.82)		
Yes	102	74 (31.09)	28 (27.18)		

'–' represented the data were analyzed using Fisher's exact test.

Table 2 Clinical characteristics and tumor marker levels of patients with benign and malignant solitary pulmonary nodules, *n* (%)

Variables	Number of cases	Benign SPNs (*n*=113)	Malignant SPNs (*n*=125)	Z/χ^2	*P*
Age, years, *M* (Q_{25}, Q_{75})		58.00 (54.00, 63.00)	62.00 (56.00, 67.00)	−3.215	0.001
Gender				10.304	0.001
Male	113	66 (58.41)	47 (37.60)		
Female	125	47 (41.59)	78 (62.40)		
Smoking history				9.405	0.002
No	168	69 (61.06)	99 (79.20)		
Yes	70	44 (38.94)	26 (20.80)		
History of malignant neoplasm				–	0.499
No	236	113 (100.00))	123 (98.40)		
Yes	2	0 (0)	2 (1.60)		
Comorbidity				2.073	0.150
No	164	83 (73.45)	81 (64.80)		
Yes	74	30 (26.55)	44 (35.20)		
CEA, μg/L, *M* (Q_{25}, Q_{75})		2.50 (1.40, 3.19)	1.91 (1.36, 2.88)	2.130	0.033
NSE, μg/L, *M* (Q_{25}, Q_{75})		11.20 (10.10, 12.60)	12.07 (10.40, 14.10)	−2.195	0.028
CYFRA21-1, ng/mL, *M* (Q_{25}, Q_{75})		2.95 (2.10, 3.80)	2.53 (2.08, 3.70)	1.413	0.158
CA125, U/mL, *M* (Q_{25}, Q_{75})		10.33 (6.95, 12.70)	9.52 (6.51, 11.50)	1.346	0.178
CA199, U/mL, *M* (Q_{25}, Q_{75})		8.60 (5.20, 10.10)	6.90 (4.90, 9.10)	1.238	0.216

'–' represented the data were analyzed using Fisher's exact test.
CA, carbohydrate antigen; CEA, carcinoembryonic antigen; CYFRA21-1, cytokeratin fragment antigen 21-1; NSE, neuron-specific enolase; SNPs, solitary pulmonary nodules.

Table 3 Imaging features of patients with benign and malignant solitary pulmonary nodules, *n* (%)

Variables	Number of cases	Benign SPNs (*n*=113)	Malignant SPNs (*n*=125)	Z/χ^2	*P* value
Nodule size, cm, *M* (Q_{25}, Q_{75})		1.90 (1.10, 2.80)	1.60 (1.10, 2.30)	1.627	0.104
Nodule location				10.482	0.033
Left upper lobe	69	36 (31.86)	33 (26.40)		
Left lower lobe	41	21 (18.58)	20 (16.00)		
Right upper lobe	66	23 (20.35)	43 (34.40)		
Right middle lobe	19	14 (12.39)	5 (4.00)		
Right lower lobe	43	19 (16.81)	24 (19.20)		
Smoothing				34.655	<0.001
No	201	79 (69.91)	122 (97.60)		
Yes	37	34 (30.09)	3 (2.40)		
Spiculation				11.438	<0.001
No	66	43 (38.05)	23 (18.40)		
Yes	172	70 (61.95)	102 (81.60)		
Lobulation				23.655	<0.001
No	195	107 (94.69)	88 (70.40)		
Yes	43	6 (5.31)	37 (29.60)		
Vascular convergence sign				65.500	<0.001
No	81	68 (60.18)	13 (10.40)		
Yes	157	45 (39.82)	112 (89.60)		
Pleural indentation				1.399	0.237
No	166	83 (73.45)	83 (66.40)		
Yes	72	30 (26.55)	42 (33.60)		
Air bronchogram				11.306	<0.001
No	207	107 (94.69)	100 (80.00)		
Yes	31	6 (5.31)	25 (20.00)		
Ground-glass opacity				74.997	<0.001
No	154	105 (92.92)	49 (39.20)		
Yes	84	8 (7.08)	76 (60.80)		
Vacuole sign				28.974	<0.001
No	174	101 (89.38)	73 (58.40)		
Yes	64	12 (10.62)	52 (41.60)		
Calcification				8.724	0.003
No	227	103 (91.15)	124 (99.20)		
Yes	11	10 (8.85)	1 (0.80)		

SPNs, solitary pulmonary nodules.

Assessment of the model calibration

The model calibration was assessed based on the training and verification groups. Hosmer–Lemeshow goodness of fit test showed a better calibration in the training group ($\chi^2=3.600$; $P=0.892$) and the verification group ($\chi^2=4.375$; $P=0.822$). In addition, the calibration curves also indicated that the model had a better calibration (Fig. 2).

Discussion

CT has long been recognized as the most sensitive and widespread imaging method in the detection and diagnosis of SPNs, especially the MDCT. For depicting pulmonary nodules, MDCT is more sensitive than single-detector CT due to its higher contrast and spatial resolution (Truong *et al.*, 2014). Although ^{18}F-fluorodeoxyglucose PET imaging of focal lesions plus CT scan is thought to

Table 4 Multivariate logistic regression analysis of benign and malignant solitary pulmonary nodules

Variables	β	S.E.	Wald	*P* value	OR	95% CI	
						Upper	Lower
Constant	−5.368	1.279	17.607	<0.001			
Age, years	0.055	0.020	7.833	0.005	1.056	1.016	1.097
Gender (female vs. male)	1.012	0.326	9.622	0.002	2.750	1.451	5.212
Nodule location							
Left lower lobe vs. left upper lobe	0.341	0.480	0.504	0.478	1.406	0.549	3.601
Right upper lobe vs. left upper lobe	1.302	0.438	8.835	0.003	3.677	1.558	8.675
Right middle lobe vs. left upper lobe	−0.204	0.677	0.091	0.763	0.815	0.216	3.073
Right lower lobe vs. left upper lobe	0.826	0.481	2.949	0.086	2.283	0.890	5.857
Spiculation (yes vs. no)	1.208	0.368	10.796	0.001	3.347	1.628	6.880
Vacuole sign (yes vs. no)	2.164	0.428	25.594	<0.001	8.706	3.765	20.134
CEA, μg/L	−0.054	0.024	5.117	0.024	0.948	0.905	0.993

CEA, carcino-embryonic antigen; CI, confidence interval; OR, odds ratio; SE, standard error.

Table 5 Diagnostic values of each model

Model	AUC	95% CI	Sensitivity	Specificity	Youden index	Cut-off	*Z*	*P* value
CEA	0.580	0.515–0.643	72.00	47.79	0.20	2.65	5.565	<0.001
Age	0.621	0.556–0.683	36.80	84.96	0.22	64	5.148	<0.001
The model without CEA	0.793	0.736–0.842	68.00	77.88	0.46	0.55	2.189	0.029
The model with CEA	0.818	0.763–0.865	64.80	84.96	0.50	0.61		

AUC, area under the curve; CEA, carcinoembryonic antigen; CI, confidence interval.

be a well-established technique for assessing ambiguous lesions more than 1 cm, it has the major limitations of unreliable imaging for nodules less than 1 cm, low sensitivity to ground-class nodules and a high cost (Herder *et al.*, 2004; Nomori *et al.*, 2004; Paśnik *et al.*, 2017). In the present study, MDCT was used to describe the imaging features of 341 patients with SPNs, and a risk prediction model for SPNs was developed based on the patients' imaging, clinical characteristics and serum tumor marker levels. Multivariate Logistic regression model showed that age, gender, nodule location, spiculation and vacuole sign were the independent risk factors for malignant SPNs, whereas serum CEA level was a protective factor. Based on this, a risk prediction model for SPNs was established: $Y = -5.368 + 0.055 \times \text{age} + 1.012 \times \text{gender (female} = 1, \text{ male} = 0) + 1.302 \times \text{nodule location (right upper lobe} = 1, \text{ others} = 0) + 1.208 \times \text{spiculation (yes} = 1, \text{ no} = 0) + 2.164 \times \text{vacuole sign (yes} = 1, \text{ no} = 0) - 0.054 \times \text{CEA}$; $P = \frac{e^Y}{1+e^Y}$, which was confirmed to have better accuracy and internal stability in predicting the probability of malignancy.

Generally, the older the patients, the higher the risk of developing tumors. The time of tumorigenic factors acting on the body is prolonged with age, leading to an increased probability of developing tumors, and the lung cancer is no exception (Toomes *et al.*, 1983; Erasmus *et al.*, 2000). Yankelevitz *et al.* (1999) found that the patients with SPNs aged over 40 years were related to a higher risk of lung cancer. Our results demonstrated that age was independent risk factors for malignant SPNs, and was involved in the establishment of the model, which was supported by several mathematical models including the Veterans Affairs model and Mayo Clinic model (Swensen *et al.*, 1997; Gould *et al.*, 2007). However, gender was not included in the above models. According to the presence or absence of spiculation, two prediction models for malignant SPNs developed in a prospective study suggested that the female was a risk factor for malignancy, with ORs of 1.76 and 1.82, respectively (McWilliams *et al.*, 2013). In the present study, gender was found to be a significant risk factor for malignant SPNs, and the probability of malignancy in females was 2.750 folds higher than that in males, slightly higher than the OR of 2.103 in another study (Wang *et al.*, 2018a). Previous evidence showed that the common pathological pattern of non-small cell lung cancer in most females, especially young females, was lung adenocarcinoma, and the proportion of lung adenocarcinoma could come up to 80% in Asian females with lung cancer (Subramanian *et al.*, 2010; Hu and Li, 2012).

In the present study, the nodule location (right upper lobe), presence of spiculation and vacuole sign as the significant risk factors for malignant SPNs were all enrolled in the prediction model. The evidence has affirmed that numerous primary malignant pulmonary nodules are placed in the upper lobes, especially in the right, although 2/3 of metastatic nodules have an impact on the lower lobes (Khan *et al.*, 2011). The risk of malignancy in the right upper lobe was the highest, approximately accounting for 45% of all malignant modules (Horeweg *et al.*, 2013). It may be explained by increased airflow into the right upper lobe during the initial inspiration and thereby increased exposure to inhaled carcinogens (Horeweg *et al.*, 2013; Cruickshank *et al.*, 2019). In addition, malignant nodules usually present with irregular, spiculated or lobulated margins because of malignant cells spreading into the pulmonary interstitium, whereas benign nodules

tend to have smooth, rounded edges (Choromańska and Macura, 2012). Spiculation is pathologically associated with desmoplastic reactions and may also be caused by the infiltration of interstitial planes and lymphatics by tumor (Khan *et al.*, 2011). Enormous evidence have demonstrated a strong association between spiculated margins and malignant pulmonary nodules (Ost and Gould 2012; Hu *et al.*, 2016; Ferreira *et al.*, 2018). Vacuole sign, unlike air bronchogram, is the area of low attenuation owing to small patent air containing bronchi in nodules. The presence of vacuole sign is also reported to be correlated with malignant pulmonary nodules (Snoeckx *et al.*, 2018; Yu *et al.*, 2020). In most studies, nodule size is found to be important in the prediction of benign and malignant SPNs (Yu *et al.*, 2020; Wang et al., 2018a,b). However, in the present study, it was not identified as a parameter of the model, which might be associated with study populations and sample size.

A prediction model for malignant SPNs that had been affirmed to have better diagnostic accuracy, internal stability and calibration was developed in the present study, with several potential implications. First, unlike most prediction models for malignant pulmonary nodules, the serum tumor marker was included in this model to further improve the diagnostic accuracy. This model was demonstrated to have the AUC of 0.818 and a better internal stability using the data of verification group. Second, the data from this model were easy to be obtained in clinic, which may help the clinicians to rapidly evaluate the probability of malignancy. Third, it was of great significance to enhance the recognition of patients at high risk of malignancy through this prediction model. Although the high proportion of nonsmokers (67.4%) in our study was similar as several Chinese studies, it was not representative for other countries (Gould *et al.*, 2013; Truong *et al.*, 2014; Yu *et al.*, 2020). Additionally, the establishment of the model was based on a retrospective study with relatively small sample sizes; the model was not simply enough for clinician use and lack of external validation. In the future, external

Fig. 1

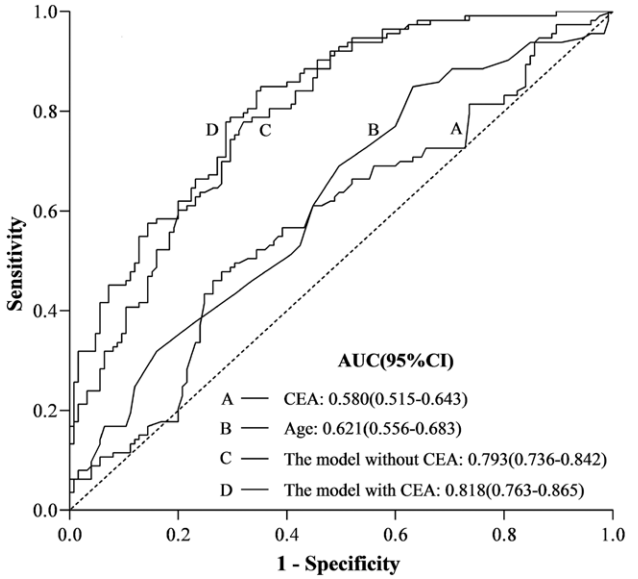

The receiver operating characteristic curves of the CEA level, age, the models with CEA and without CEA. CEA, carcinoembryonic antigen.

Table 6 Verification of the prediction model

	Actual condition			
Prediction model	Benign	Malignant	χ^2	*P* value
Benign	35 (71.43)	19 (35.19)	0.758	0.384
Malignant	14 (28.57)	35 (64.81)		

Fig. 2

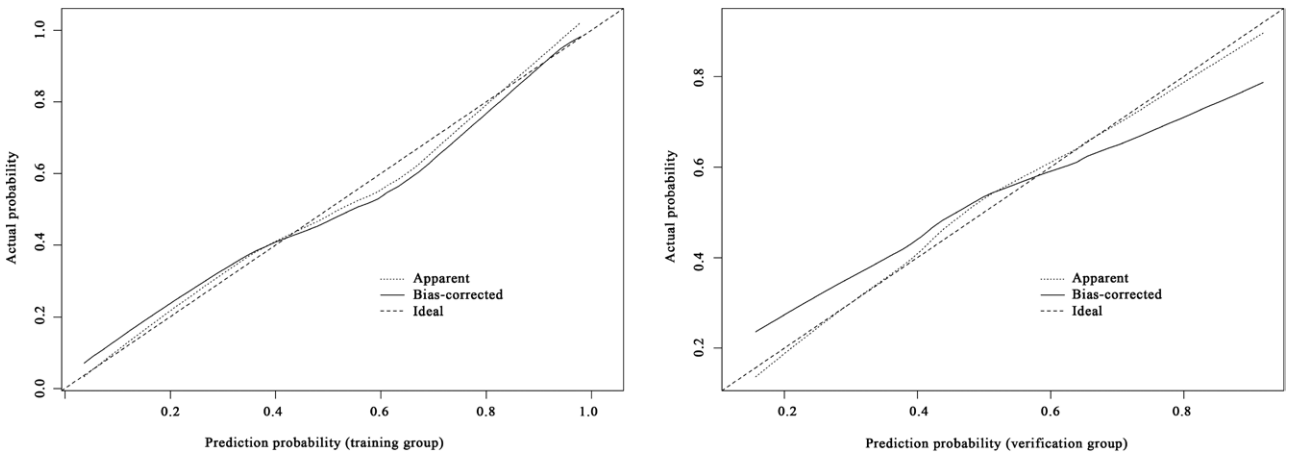

The calibration curves of the prediction model.

validation will be further implemented in large-scale, prospective studies.

Conclusion

The influencing factors for malignant SPNs include age, gender, nodule location, spiculation, vacuole sign and CEA level, based on which a prediction model is established. It is demonstrated to have better accuracy and internal stability in predicting the probability of malignancy for SPNs.

Acknowledgements

This research did not receive any specific grant from funding agencies in the public, commercial, or not-for-profit sectors. This study was performed based on the principle of Helsinki Declaration and was approved by the Institutional Review Board of Weihai Central Hospital (approval No.: WHSZXYYKYLL-2020-03)..

Conflicts of interest

There are no conflicts of interest.

References

Borghesi A, Michelini S, Golemi S, Scrimieri A, Maroldi R (2020). What's new on quantitative CT analysis as a tool to predict growth in persistent pulmonary subsolid nodules? A literature review. *Diagnostics (Basel)* **10**:E55.

Callister ME, Baldwin DR, Akram AR, Barnard S, Cane P, Draffan J, *et al.*; British Thoracic Society Pulmonary Nodule Guideline Development Group; British Thoracic Society Standards of Care Committee (2015). British Thoracic Society guidelines for the investigation and management of pulmonary nodules. *Thorax* **70** (Suppl 2):ii1–ii54.

Choromańska A, Macura KJ (2012). Evaluation of solitary pulmonary nodule detected during computed tomography examination. *Pol J Radiol* **77**:22–34.

Chung K, Mets OM, Gerke PK, Jacobs C, den Harder AM, Scholten ET, *et al.* (2018). Brock malignancy risk calculator for pulmonary nodules: validation outside a lung cancer screening population. *Thorax* **73**:857–863.

Cruickshank A, Stieler G, Ameer F (2019). Evaluation of the solitary pulmonary nodule. *Intern Med J* **49**:306–315.

Erasmus JJ, McAdams HP, Connolly JE (2000). Solitary pulmonary nodules: part II. Evaluation of the indeterminate nodule. *Radiographics* **20**:59–66.

Ferreira JR Jr, Oliveira MC, de Azevedo-Marques PM (2018). Characterization of pulmonary nodules based on features of margin sharpness and texture. *J Digit Imaging* **31**:451–463.

Gould MK, Ananth L, Barnett PG; Veterans Affairs SNAP Cooperative Study Group (2007). A clinical model to estimate the pretest probability of lung cancer in patients with solitary pulmonary nodules. *Chest* **131**:383–388.

Gould MK, Donington J, Lynch WR, Mazzone PJ, Midthun DE, Naidich DP, *et al.* (2013). Evaluation of individuals with pulmonary nodules: when is it lung cancer? Diagnosis and management of lung cancer, 3rd ed: American college of chest physicians evidence-based clinical practice guidelines. *Chest* **143** (5 Suppl): e93S–e120S.

Herder GJ, Golding RP, Hoekstra OS, Comans EF, Teule GJ, Postmus PE, Smit EF (2004). The performance of(18)F-fluorodeoxyglucose positron emission tomography in small solitary pulmonary nodules. *Eur J Nucl Med Mol Imaging* **31**:1231–1236.

Horeweg N, van der Aalst CM, Thunnissen E, Nackaerts K, Weenink C, Groen HJ, *et al.* (2013). Characteristics of lung cancers detected by computer tomography screening in the randomized NELSON trial. *Am J Respir Crit Care Med* **187**:848–854.

Hu CP, Li M (2012). Overview of female non-small cell lung cancer. *Chin J Tuberc Respir Dis* **35**:89–90.

Hu H, Wang Q, Tang H, Xiong L, Lin Q (2016). Multi-slice computed tomography characteristics of solitary pulmonary ground-glass nodules: differences between malignant and benign. *Thorac Cancer* **7**:80–87.

Khan AN, Al-Jahdali HH, Irion KL, Arabi M, Koteyar SS (2011). Solitary pulmonary nodule: a diagnostic algorithm in the light of current imaging technique. *Avicenna J Med* **1**:39–51.

Kikano GE, Fabien A, Schilz R (2015). Evaluation of the solitary pulmonary nodule. *Am Fam Physician* **92**:1084–1091.

Larici AR, Farchione A, Franchi P, Ciliberto M, Cicchetti G, Calandriello L, *et al.* (2017). Lung nodules: size still matters. *Eur Respir Rev* **26**:170025.

Li X, Zhang Q, Jin X, Cao L (2017). Combining serum miRNAs, CEA, and CYFRA21-1 with imaging and clinical features to distinguish benign and malignant pulmonary nodules: a pilot study: Xianfeng Li *et al.*: combining biomarker, imaging, and clinical features to distinguish pulmonary nodules. *World J Surg Oncol* **15**:107.

MacMahon H, Austin JH, Gamsu G, Herold CJ, Jett JR, Naidich DP, *et al.*; Fleischner Society. (2005). Guidelines for management of small pulmonary nodules detected on CT scans: a statement from the Fleischner Society. *Radiology* **237**:395–400.

MacMahon H, Naidich DP, Goo JM, Lee KS, Leung ANC, Mayo JR, *et al.* (2017). Guidelines for management of incidental pulmonary nodules detected on CT images: from the Fleischner Society 2017. *Radiology* **284**:228–243.

McWilliams A, Tammemagi MC, Mayo JR, Roberts H, Liu, G, Soghrati K, *et al.* (2013). Probability of cancer in pulmonary nodules detected on first screening CT. *N Engl J Med* **369**:910–919.

Naidich DP, Bankier AA, MacMahon H, Schaefer-Prokop CM, Pistolesi M, Goo JM, *et al.* (2013). Recommendations for the management of subsolid pulmonary nodules detected at CT: a statement from the Fleischner Society. *Radiology* **266**:304–317.

Nomori H, Watanabe K, Ohtsuka T, Naruke T, Suemasu K, Uno K (2004). Evaluation of F-18 fluorodeoxyglucose (FDG) PET scanning for pulmonary nodules less than 3 cm in diameter, with special reference to the CT images. *Lung Cancer* **45**:19–27.

Ost DE, Gould MK (2012). Decision making in patients with pulmonary nodules. *Am J Respir Crit Care Med* **185**:363–372.

Paśnik M, Bestry I, Roszkowski-Śliż K (2017). Solitary pulmonary nodule – the role of imaging in the diagnostic process. *Adv Respir Med* **85**:345–351.

Patel VK, Naik SK, Naidich DP, Travis WD, Weingarten JA, Lazzaro R, *et al.* (2013). A practical algorithmic approach to the diagnosis and management of solitary pulmonary nodules: part 1: radiologic characteristics and imaging modalities. *Chest* **143**:825–839.

Snoeckx A, Reyntiens P, Desbuquoit D, Spinhoven MJ, Van Schil PE, van Meerbeeck JP, Parizel PM (2018). Evaluation of the solitary pulmonary nodule: size matters, but do not ignore the power of morphology. *Insights Imaging* **9**:73–86.

Subramanian J, Morgensztern D, Goodgame B, Baggstrom MQ, Gao F, Piccirillo J, Govindan R (2010). Distinctive characteristics of non-small cell lung cancer (NSCLC) in the young: a surveillance, epidemiology, and end results (SEER) analysis. *J Thorac Oncol* **5**:23–28.

Swensen SJ, Silverstein MD, Ilstrup DM, Schleck CD, Edell ES (1997). The probability of malignancy in solitary pulmonary nodules. Application to small radiologically indeterminate nodules. *Arch Intern Med* **157**:849–855.

Toomes H, Delphendahl A, Manke HG, Vogt-Moykopf I (1983). The coin lesion of the lung. A review of 955 resected coin lesions. *Cancer* **51**:534–537.

Truong MT, Ko JP, Rossi SE, Rossi I, Viswanathan C, Bruzzi JF, *et al.* (2014). Update in the evaluation of the solitary pulmonary nodule. *Radiographics* **34**:1658–1679.

Wahidi MM, Govert JA, Goudar RK, Gould MK, McCrory DC; American College of Chest Physicians (2007). Evidence for the treatment of patients with pulmonary nodules: when is it lung cancer?: ACCP evidence-based clinical practice guidelines (2nd ed). *Chest* **132**:94S–107S.

Wang L, Chen Y, Tang K, Lin J, Zhang H (2018a). The value of 18F-FDG PET/CT mathematical prediction model in diagnosis of solitary pulmonary nodules. *Biomed Res Int* **2018**:9453967.

Wang X, Xu YH, Du ZY, Qian YJ, Xu ZH, Chen R *et al.* (2018b). Risk factor analysis of the patients with solitary pulmonary nodules and establishment of a prediction model for the probability of malignancy. *Chin J Oncol* **40**:115–120.

Yankelevitz DF, Gupta R, Zhao B, Henschke CI (1999). Small pulmonary nodules: evaluation with repeat CT–preliminary experience. *Radiology* **212**:561–566.

Yu M, Wang Z, Yang G, Cheng Y (2020). A model of malignant risk prediction for solitary pulmonary nodules on 18 F-FDG PET/CT: building and estimating. *Thorac Cancer* **11**:1211–1215.